

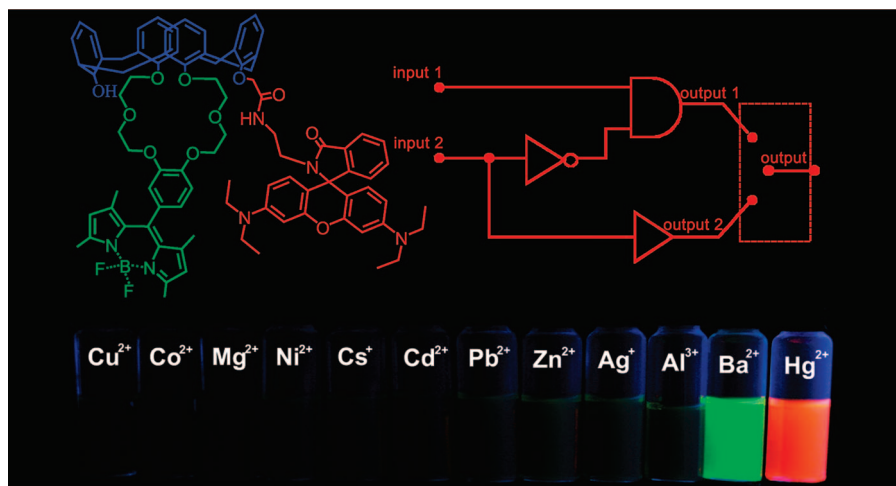
## A Multianalyte Chemosensor on a Single Molecule: Promising Structure for an Integrated Logic Gate

Mingjian Yuan, Weidong Zhou, Xiaofeng Liu, Mei Zhu, Junbo Li, Xiaodong Yin, Haiyan Zheng, Zicheng Zuo, Canbin Ouyang, Huibiao Liu, Yuliang Li,\* and Daoben Zhu

Beijing National Laboratory for Molecular Science (BNLMS), CAS Key Laboratory of Organic Solids, Institute of Chemistry, Chinese Academy of Sciences and Graduate School of Chinese Academy of Sciences, Beijing 100190, People's Republic of China

ylli@iccas.ac.cn

Received March 12, 2008



A novel fluorescent probe that possess both BODIPY and Rhodamine moieties has been designed for the selective detection of  $\text{Hg}^{2+}$  and  $\text{Ba}^{2+}$  ions on the controlling by a logic gate. The characteristic fluorescence of the  $\text{Ba}^{2+}$ -selective OFF–ON and the  $\text{Hg}^{2+}$ -selective fluorescence bathochromic shift can be observed, and the concept has been used to construct a combinational logic circuit at the molecular level. These results will be useful for further molecular design to mimic the function of the complex logic gates on controlling.

### Introduction

The urge for miniaturization is encouraging the design of molecular-level electronic devices.<sup>1</sup> Since the pioneering work by de Silva,<sup>2</sup> remarkable progress has been made in the development of molecular logic gates. Various molecular logic gates (AND, OR, XOR, INHIBIT, NAND, half-adder, half-subtractor) have been well studied.<sup>3</sup> However, most of the molecular logic gates reported so far performed a single

transduction step<sup>4</sup> that molecular switch converts initial input into the output by a very simple chemical process.<sup>5</sup> The lack of channel to exchange signals between independent molecular components has limited the development of multistep transduction mechanisms. So the communication of signals at the

(1) (a) Balzani, V.; Credi, A.; Venturi, M. *Molecular Devices and Machines: A Journey into the Nanoworld*; Wiley-VCH: Weinheim, Germany, 2003. (b) Feringa, B. L. *Molecular Switches*; Wiley-VCH: Weinheim, Germany, 2001. (c) Credi, A. *Angew. Chem., Int. Ed.* **2007**, *46*, 2.

(2) de Silva, A. P.; Gunaratne, H. Q. N.; McCoy, C. P. *Nature*. **1993**, *364*, 42.

(3) (a) de Silva, A. P.; de Silva, S. S. K.; Goonesekera, N. C. W.; Gunaratne, H. Q. N.; Lynch, P. L. M.; Nesbitt, K. R.; Patuwathaviathana, S. T.; Ramyalal, N. L. D. S. *J. Am. Chem. Soc.* **2007**, *129*, 3050. (b) Tang, Y.; He, F.; Wang, S.; Li, Y.; Zhu, D.; Bazan, G. C. *Adv. Mater.* **2006**, *18*, 2105. (c) Andreasson, J.; Kodis, G.; Terazono, Y.; Liddell, P. A.; Bandyopadhyay, S.; Mitchell, R. H.; Moore, T. A.; Gust, D. *J. Am. Chem. Soc.* **2004**, *126*, 15926. (d) Margulies, D.; Felder, C. E.; Melman, G.; Shanzer, A. *J. Am. Chem. Soc.* **2007**, *129*, 347. (e) Qu, D. H.; Wang, Q. C.; Tian, H. *Angew. Chem., Int. Ed.* **2005**, *44*, 5296. (f) Coskun, A.; Deniz, E.; Akkaya, E. U. *Org. Lett.* **2005**, *7*, 5187. (g) Guo, X.; Zhang, D.; Zhou, Y.; Zhu, D. *J. Org. Chem.* **2003**, *68*, 5681.

(4) Raymo, F. M.; Alvarado, R. J.; Giordani, S.; Cejas, M. A. *J. Am. Chem. Soc.* **2003**, *125*, 2361.

(5) Raymo, F. M.; Giordani, S. *Org. Lett.* **2001**, *3*, 1833.

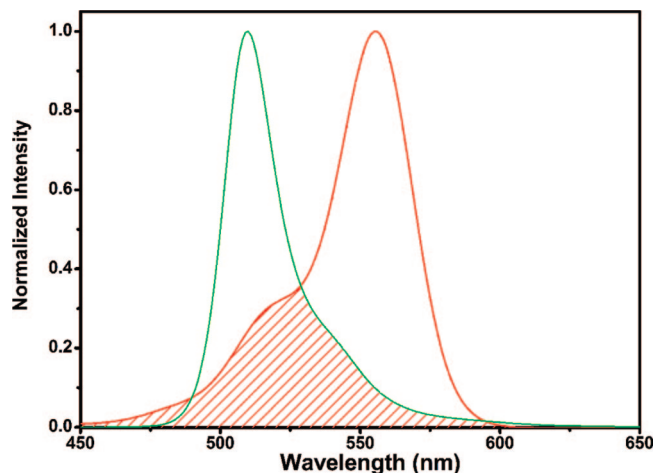


**FIGURE 1.** Spectral overlap between BODIPY emission (green) and ring-opened Rhodamine B absorption (red).

molecular level between independent components is very important and is necessary in the development of innovative material for data storage and processing.

Currently, the fluorescence resonance energy transfer (FRET) is drawing particular interesting due to potential benefits in the signal communication process.<sup>6</sup> FRET rises from an interaction between a pair of fluorophores in their excited states, thus it is an effective mechanism for regulating the states of fluorophore.<sup>7</sup> In fact, the fluorescence intensity of the independent fluorophore is able to tune by the controlling FRET process in response to external stimulants, so the corresponding molecular-level signals communication device can be constructed.

Rhodamine-based dyes have been widely used for conjugation with biomolecules, owing to their excellent spectroscopic properties such as large molar extinction coefficient and high fluorescence quantum yield.<sup>8</sup> Moreover, it is well-known that many derivatives of Rhodamine undergo equilibrium between spiroactam and ring-opened amide, and the two forms always behave with completely different spectroscopic properties.<sup>9</sup> BODIPY is another very attractive functional group for construction of a molecular sensor because of its advantageous characteristics, such as high extinction coefficients, high quantum yield, and the fact that its excitation wavelength lies in the visible-wavelength range.<sup>10</sup> As shown in Figure 1, BODIPY shows the emission in the range of 500–550 nm, and hence the overlap between its emission spectra and the absorption spectra of the ring-opened form of Rhodamine is significantly large. By contrast, there is almost no overlap between the emission spectra of BODIPY and the absorption spectra of spiroactam form Rhodamine. As we mentioned, the two states

of Rhodamine dyes show different absorption spectra, thus it is possible to regulate the fluorescence state of a system by irradiating a molecule containing both Rhodamine and BODIPY. Consequently, for the BODIPY–Rhodamine system the corresponding PET (photoinduced electron transfer) and FRET process as well as “output” signals can be modulated.

Calixarene has been thoroughly investigated as the framework of many fluorescent chemosensors due to its flexible structural property.<sup>11</sup> Owing to the pioneering work by Kim and co-workers,<sup>12</sup> calixarene has also been proven to be an effective platform for the FRET process.

Keeping these thoughts in mind, we speculated the attachment of both BODIPY and Rhodamine groups to calix[4]arene could promise a system where there is a FRET from a fluorescence donor to a nearby acceptor, then the system’s fluorescence can be modulated with different stimulations. We linked the BODIPY group to calix[4] arene through a crown-6 loop, which is capable of binding the main-group ions effectively. Besides, we attach a spiroactam-formed Rhodamine group through the chloroacetyl-ethylenediamine moiety to the calix[4]arene framework and we confer this structure may give a stable binding mode for some specific cations.

## Results and Discussion

The preparation of chemosensor **1** was depicted in Scheme 1. Treatment of Rhodamine B–ethylenediamine (compound **2**) with chloroacetyl chloride in anhydrous  $\text{CH}_2\text{Cl}_2$  gave compound **3** in a yield of 90%. Compound **5** was obtained by reaction of compound **4** with 2,4-dimethylpyrrol with TFA as catalyst followed by oxidizing with DDQ and treatment with  $\text{BF}_3 \cdot \text{Et}_2\text{O}$  in 35% yield. Reaction of calix[4]arene with compound **5** by using *t*-BuOK as a base in benzene gave compound **6** in 40% yield. Synthesis of compound **1** was preformed by the condensation of *N*-(rhodamine-B)lactam-ethyl-2-chloroacetamide (**3**) with *cone*-calix[4]monocrown-6 (**6**) in the presence of  $\text{Cs}_2\text{CO}_3$  as a base and a catalytic amount of KI in a yield of 20%.

The structure of **1–6** was characterized by  $^1\text{H}$  NMR,  $^{13}\text{C}$  NMR, and MALDI-TOF MS. The spiroactam form of the Rhodamine unit in compound **1** was confirmed by the characteristic peak of the 9-carbon of xanthenes in **1** near 66 ppm in the  $^{13}\text{C}$  NMR spectrum.<sup>13</sup>

As designed, in this paper we demonstrated a new concept of how the communication of optical signals between two independent molecular switches can be established, and these processes can be analyzed with the combinational logic circuit. To modulate the systems different fluorescence states, we take advantage of the FRET process between BODIPY and Rhodamine groups in combination with the isomerization of the two states of Rhodamines. As shown in Figure 2, the stimulations inducing the interconversion between four states for controlling the system’s fluorescence states could be realized. (a) As a fluorescence donor the spectrum of BODIPY exhibits very weak emission due to the PET process. (b) When one specific ion

(6) (a) Julius, R.; Onagl, H. *Chem. Commun.* **2005**, 4604. (b) Margulies, D.; Melman, G.; Felder, C. E.; Arad-Yellin, R.; Shanzler, A. *J. Am. Chem. Soc.* **2004**, *126*, 15400. (c) Li, Y.; Li, H.; Li, Y.; Liu, H.; Wang, S.; He, X.; Wang, N.; Zhu, D. *Org. Lett.* **2005**, *7*, 4835.

(7) Fister, T. *Ann. Phys.* **1948**, *2*, 55.

(8) Dujols, V.; Ford, F.; Czarnik, A. W. *J. Am. Chem. Soc.* **1997**, *119*, 7386.

(9) (a) Yang, Y.; Yook, K.; Tae, J. *J. Am. Chem. Soc.* **2005**, *127*, 16760. (b) Kwon, J. K.; Jang, Y. J.; Lee, Y. J.; Kim, K. M.; Seo, M. S.; Nam, W.; Yoon, J. *J. Am. Chem. Soc.* **2005**, *127*, 10107. (c) Zheng, H.; Qian, Z.; Xu, L.; Yuan, F.; Lan, L.; Xu, J. *Org. Lett.* **2006**, *8*, 859. (d) Xiang, Y.; Tong, A. *Org. Lett.* **2006**, *8*, 1549. (e) Wu, J.; Hwang, I.; Kim, K. S.; Kim, J. S. *Org. Lett.* **2007**, *9*, 907.

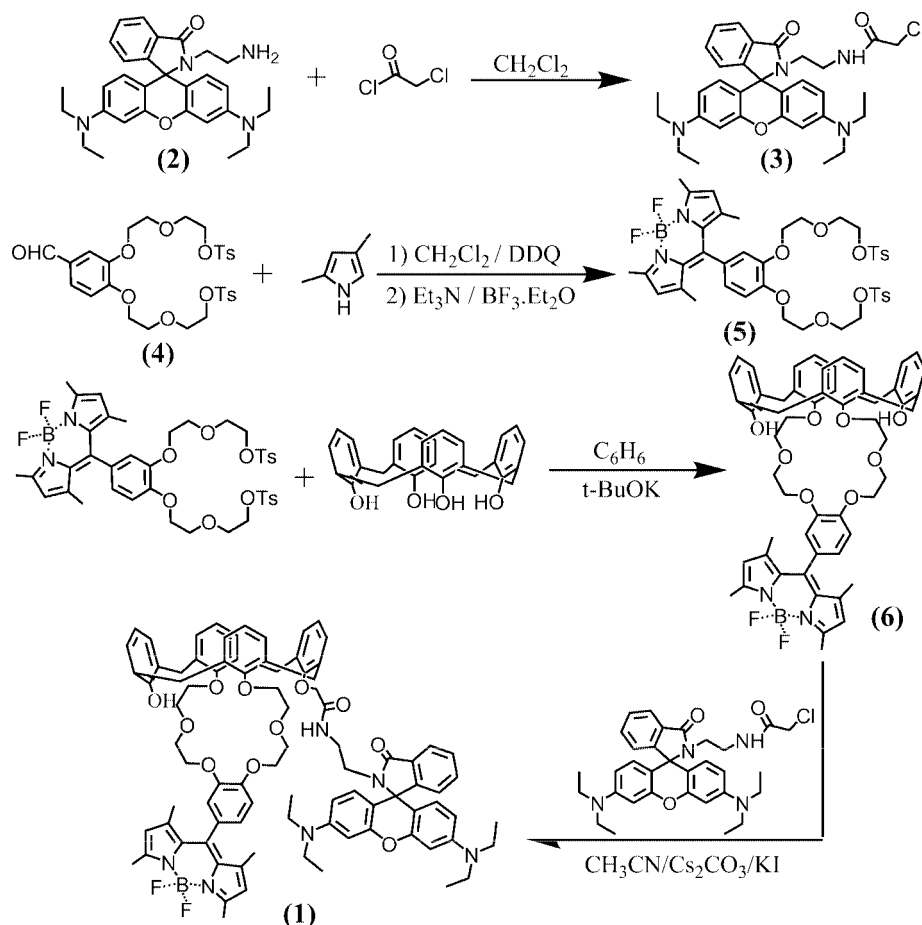
(10) (a) Haugland, R. P. *Handbook of Fluorescent Probes And Research Chemicals*, 9th ed.; Molecular Probe Inc.: Eugene, OR, 2002. (b) Rurack, K.; Kollmannsberger, M.; Daub, J. *Angew. Chem., Int. Ed.* **2001**, *40*, 385. (c) Yoon, S.; Albers, A. E.; Wong, A. P.; Chang, C. J. *J. Am. Chem. Soc.* **2005**, *127*, 16030. (d) Coskun, A.; Akkaya, E. U. *J. Am. Chem. Soc.* **2005**, *127*, 10464.

(11) (a) Kim, J. S.; Quang, D. T. *Chem. Rev.* **2007**, *107*, 3780. (b) Chang, K. C.; Su, I.; Senthilvelan, A.; Chung, W. S. *Org. Lett.* **2007**, *9*, 3363. (c) Kim, S. K.; Lee, S. H.; Lee, J. Y.; Lee, J. Y.; Bartsch, R. A.; Kim, J. S. *J. Am. Chem. Soc.* **2004**, *126*, 16499.

(12) (a) Lee, M. H.; Quang, D. T.; Jung, H. S.; Yoon, J. Y.; Lee, C. H.; Kim, J. S. *J. Org. Chem.* **2007**, *72*, 4242. (b) Othman, A. B.; Lee, J. W.; Wu, J.; Kim, J. S.; Abidi, R.; Thuery, P.; Strub, J. M.; Dorssealer, A. V.; Vicens, J. *J. Org. Chem.* **2007**, *72*, 7634.

(13) Anthoni, U.; Christopherson, C.; Nielsen, P.; Puschl, A.; Schaumburg, K. *Struct. Chem.* **1995**, *3*, 161.

## SCHEME 1. Synthesis of the Calix[4]arene-Based Chemosensor 1



was added, the PET process was partially restrained then the emission at 505 nm (BODIPY) became stronger. (c) The colorless Rhodamine spirolactam state isomerizes to the red ring-opened form upon treated with another ion. The process is accompanied by the appearance of a new band in the absorption spectrum and a strong fluorescence band in the long wavelength. (d) Both ions were added inducing the PET process to be reduced and the FRET process to turn to the “on” state.

An optimized  $\text{CH}_3\text{CN}$  solution of **1** was selected for the spectral investigation. Figure 3a showed the absorption spectral changes of compound **1** as a function of the  $\text{Hg}^{2+}$  concentration in  $\text{CH}_3\text{CN}$  at room temperature. When no metal ion was added, the absorption spectra of solution **1** is characterized by only one intense band centered at 499 nm, which could be attributed to the characteristic absorbance of the BODIPY group.<sup>14</sup> Almost no other absorption above 500 nm was observed, whereas a

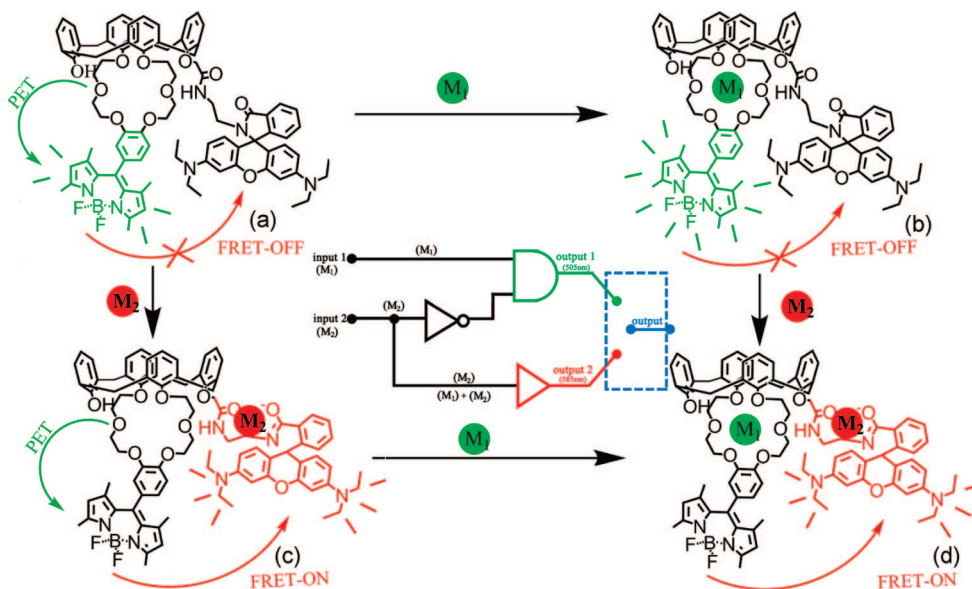
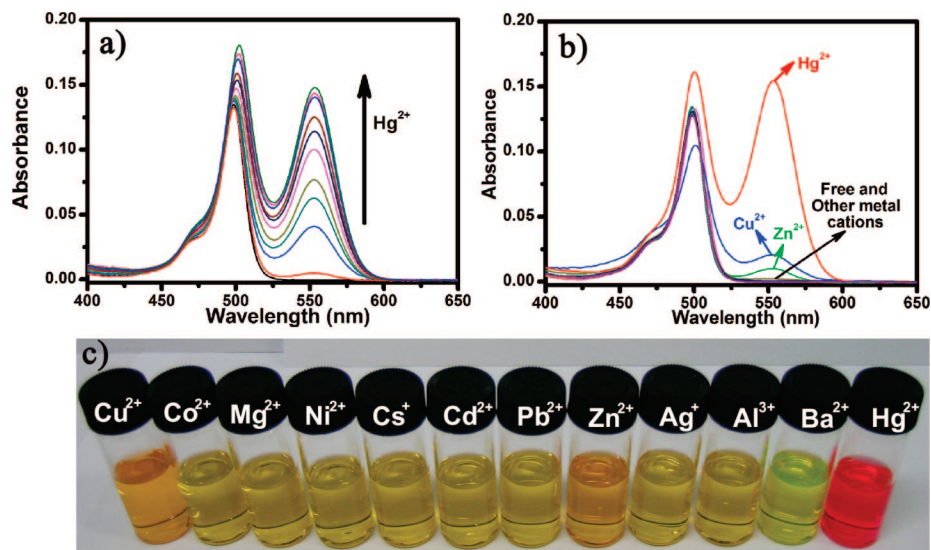
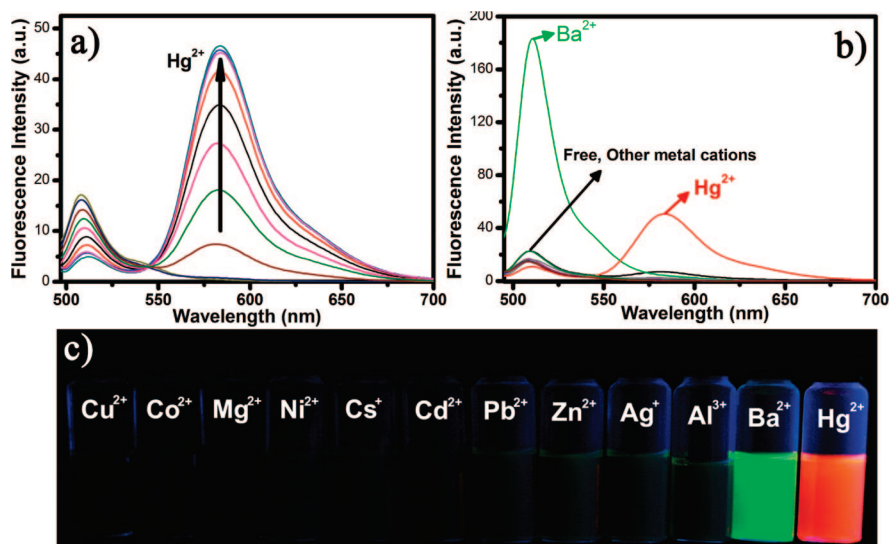


FIGURE 2. Proposed different complexation situation of compound **1** with different ions.



**FIGURE 3.** (a) Absorbance spectra of compound **1** in the presence of increasing  $\text{Hg}^{2+}$  concentrations (0, 2, 3, 3.5, 4, 5, 10, 15, 20, 30, 40  $\mu\text{M}$ ) in acetonitrile solution. The concentration of compound **1** was 2  $\mu\text{M}$ . (b) Absorbance spectra change of compound **1** (2  $\mu\text{M}$ ) upon addition of different metal cations (20 equiv) in acetonitrile solution. (c) Photograph of compound **1** with different metal ions.



**FIGURE 4.** (a) Emission spectra of compound **1** in the presence of increasing  $\text{Hg}^{2+}$  concentrations (0, 2, 3, 3.5, 4, 5, 10, 15, 20, 30, 40  $\mu\text{M}$ ) in acetonitrile solution. The concentration of compound **1** was 2  $\mu\text{M}$ . Excitation wavelength was 490 nm with 5 nm slit widths. (b) Emission spectra change of compound **1** (2  $\mu\text{M}$ ) upon addition of different metal cations (20 equiv) in acetonitrile solution. (c) Photograph of compound **1** with different metal ions under UV lights.

significant enhancement (>500-fold) of the characteristic absorption of Rhodamine emerged soon after  $\text{Hg}^{2+}$  was injected into the solution. There is a new peak located at 558 nm that can be ascribed to the delocalized xanthene moiety of Rhodamine, suggesting the clear formation of the ring-opened amide form.

The selective coordination studies of compound **1** were then extended to related heavy, transition, and main group metal ions by UV–vis spectroscopy. Figure 3b shows the representative chromogenic behavior of **1** toward metal ions in  $\text{CH}_3\text{CN}$  solution. As shown, under the identical condition, 2.0  $\mu\text{M}$  compound **1** exhibits no response to the addition of 20 equiv of metal ions such as  $\text{Co}^{2+}$ ,  $\text{Mg}^{2+}$ ,  $\text{Ni}^{2+}$ ,  $\text{Cs}^+$ ,  $\text{Cd}^{2+}$ ,  $\text{Ba}^{2+}$ ,  $\text{Ag}^+$ ,  $\text{Al}^{3+}$ , and  $\text{Pb}^{2+}$ . A very mild increase of absorbance at 553 nm was detected with the same amount of  $\text{Cu}^{2+}$  (50-fold),  $\text{Zn}^{2+}$  (30-fold), but a much longer response time was required. The  $\text{Hg}^{2+}$  sensing and the concomitant absorption changes were clearly visible to the naked eye, as can be seen in the photograph

(Figure 3c), where the yellow solution of **1** became pink-red upon titration with  $\text{Hg}^{2+}$  ions. These interesting phenomena prove that compound **1** can serve as a “naked eye” chemosensor specific for  $\text{Hg}^{2+}$ .

Furthermore, the selective fluorimetric response of **1** to all the tested metal ions was also studied. As expect, compound **1** exhibits a single fluorescence band maximum at 505 nm that could be attributed to the characteristic emission of the BODIPY group, and the fluorescence intensity is particularly low. When  $\text{Hg}^{2+}$  was added,  $\text{Hg}^{2+}$  will induce the Rhodamine group to form a ring-opened state then the typical Rhodamine’s emission band centered at 585 nm will be observed. The experiment was then conducted, as depict in Figure 4a; the emission spectra was obtained by excitation at 490 nm. Upon adding  $\text{Hg}^{2+}$  the intensity of the emission maximum at 505 nm gradually decreased following the formation of a new band centered at 585 nm, and an isosbestic point at 541nm was observed. The

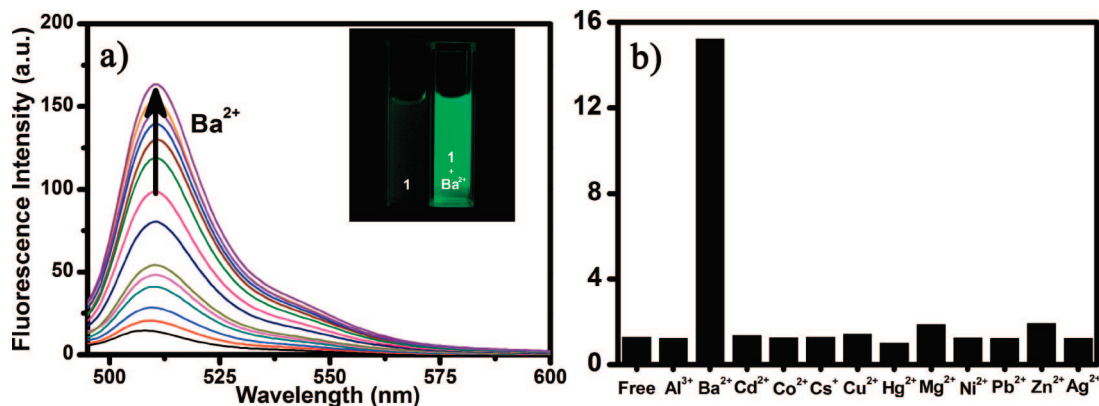


**FIGURE 5.** (a) Emission spectra of compound **1** in the presence of increasing  $\text{Ba}^{2+}$  concentrations (0, 0.4, 0.8, 1.2, 1.6, 5, 8, 10, 15, 20, 40, 50, 100  $\mu\text{M}$ ) in acetonitrile solution. Excitation wavelength was 490 nm with 5 nm slit widths. (b) Fluorescence responses of compound **1** to various metal ions (20 equiv). Bars represent the final integrated fluorescence response over the initial integrated emission.

phenomena demonstrate that we have a very efficient emission ratiometric chemosensor working in the long-wavelength region.  $\text{Hg}^{2+}$  binding induces the formation of a new emission band, the phenomena proved that an efficient FRET process takes place from the donor (BODIPY) group to the acceptor (Rhodamine) group. Under the identical condition,  $\text{Co}^{2+}$ ,  $\text{Mg}^{2+}$ ,  $\text{Ni}^{2+}$ ,  $\text{Cs}^+$ ,  $\text{Cd}^{2+}$ ,  $\text{Ag}^+$ ,  $\text{Al}^{3+}$ ,  $\text{Pb}^{2+}$ ,  $\text{Cu}^{2+}$ , and  $\text{Zn}^{2+}$  show nearly no response. Interestingly, compound **1** exhibits a 15-fold enhancement of fluorescence intensity at a peak wavelength of 505 nm in the presence of 20 equiv of  $\text{Ba}^{2+}$  and we will discuss the reason in the next section. Importantly, the large cation-induced bathochromic shift for  $\text{Hg}^{2+}$  in emission spectra results in a color change from light-green to orange. This visible emission allows  $\text{Hg}^{2+}$  to be distinguished by the naked eye under UV light (Figure 4c).

Binding analysis using the method of continuous variations (Job's plot) established a 1:1 stoichiometry for the **1**– $\text{Hg}^{2+}$  complex. Following the Benesi–Hildebrand-type analysis, the association constant  $K_a$  value was determined to be  $1.15 \times 10^5$  (Supporting Information).

To further confirm energy transfer from the BODIPY to the Rhodamine group, time-resolved nanosecond fluorescence experiments were conducted. Fluorescence decays for both compound **1** and the fully  $\text{Hg}^{2+}$ -added compound **1** were carried out in acetonitrile solution with use of the time-correlated single-photon-counting method. The samples were excited at 486 nm, and the fluorescence decay was monitored at the emission maximums: 505 nm for compound **1** and or 585 nm for the  $\text{Hg}^{2+}$ -added compound. The data were fitted by using a reconvolution method of the instrument response function (IRF) producing  $\chi^2$  fitting values of 1–1.5. The photophysical data were summarized (Supporting Information). The data suggest the occurrence of intramolecular energy transfer from excited BODIPY to Rhodamine in the molecular system. So the fluorescence quenching behavior of the BODIPY moiety can be explained in terms of the enhanced energy transfer between the two moieties and the reduced intermolecular quenching, which resulted in an increase of the emission intensity of the Rhodamine group.

Interestingly, as mentioned above, we observed the BODIPY fluorescence intensity was markedly enhanced when  $\text{Ba}^{2+}$  was added to the solution. Other ions did not induce these effects. Compound **1** is virtually weak fluorescence in the apo state that resulted from the efficient PET quenching of the excited state of the BODIPY moiety by the lone pair of electrons on the

oxygen atoms in the oxa-crown-6 loop.<sup>15</sup> Upon adding  $\text{Ba}^{2+}$ , the fluorescent intensity of **1** increases by over 15-fold accompanied by a bathochromic shift slightly to 507 nm. The fluorescence intensity enhancement could be attributed to the capture of  $\text{Ba}^{2+}$  by the receptor then resulting in the reduction of the electron-donating ability of oxygen to the BODIPY moiety, thus the PET process is partially suppressed and causes an enhancement in emission. The fluorescence intensity changes at 505 nm of compound **1** upon addition of various metal ions are listed in Figure 5. The results indicate that compound **1** shows high selectivity toward  $\text{Ba}^{2+}$  among the other ions being investigated. Binding analysis with the method of continuous variations establishes that a 1:1  $\text{Ba}^{2+}$ /**1** complex was formed. Following a Benesi–Hildebrand-type analysis, the association constant  $K_a$  was determined to be  $1.68 \times 10^5$  (Supporting Information). Thus, compound **1** can also serve as a  $\text{Ba}^{2+}$ -selective fluorescent probe with visible excitation and emission profiles, giving a 15-fold turn-on response.

The conversation process of the system with different modulators is clearly demonstrated in Figure 2. Optically dilute solutions of compound **1** in  $\text{CH}_3\text{CN}$  have a weak emission band at 505 nm. Addition of  $\text{Ba}^{2+}$  results in a CHEF (chelating enhanced fluorescence) effect and the BODIPY emission becomes strong. This is of course expected, considering the PET nature of the emission. The addition of  $\text{Hg}^{2+}$  induced the ring-opened Rhodamine state formed, and this time the emission band at 505 nm is gradually decreased and a new band at 585 nm is formed due to the efficient FRET mechanism. For both the  $\text{Ba}^{2+}$  and  $\text{Hg}^{2+}$  addition, the PET process is blocked and the FRET process turns on. The green emission is still efficiently quenched and the red emission is stronger (Figure 6).

These behaviors can be analyzed with the combinational logic circuit. The two input signals are  $I_1$  ( $\text{Ba}^{2+}$ ) and  $I_2$  ( $\text{Hg}^{2+}$ ). The output signals are Output 1 (the emission band at 505 nm of the BODIPY unit) and Output 2 (the emission band at 585 nm of the Rhodamine unit). As can be seen from the truth table (Figure 7), monitoring the fluorescence at 505 nm (output 1) upon addition of  $\text{Ba}^{2+}$ ,  $\text{Hg}^{2+}$ , and an equimolar mix of  $\text{Ba}^{2+}$  and  $\text{Hg}^{2+}$  leads to an INHIBIT<sup>16</sup> logic gate. INHIBIT is neither

(14) Gabe, Y.; Urano, Y.; Kikuchi, K.; Kojima, H.; Nagano, T. *J. Am. Chem. Soc.* **2004**, *126*, 3357.

(15) Yuan, M.; Li, Y.; Li, J.; Li, C.; Liu, X.; Lv, J.; Xu, J.; Liu, H.; Wang, S.; Zhu, D. *Org. Lett.* **2007**, *9*, 2313.

(16) Gunlaugsson, T.; Mac Donall, D. A.; Parker, D. *Chem. Commun* **2000**, 93.

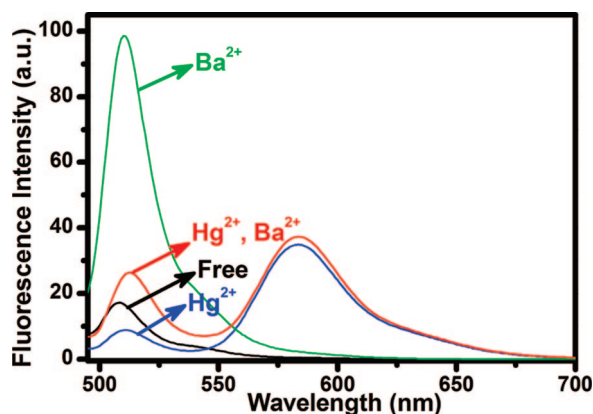


FIGURE 6. Fluorescence spectra about different complexation situations of compound **1** with  $\text{Ba}^{2+}$  and  $\text{Hg}^{2+}$ .

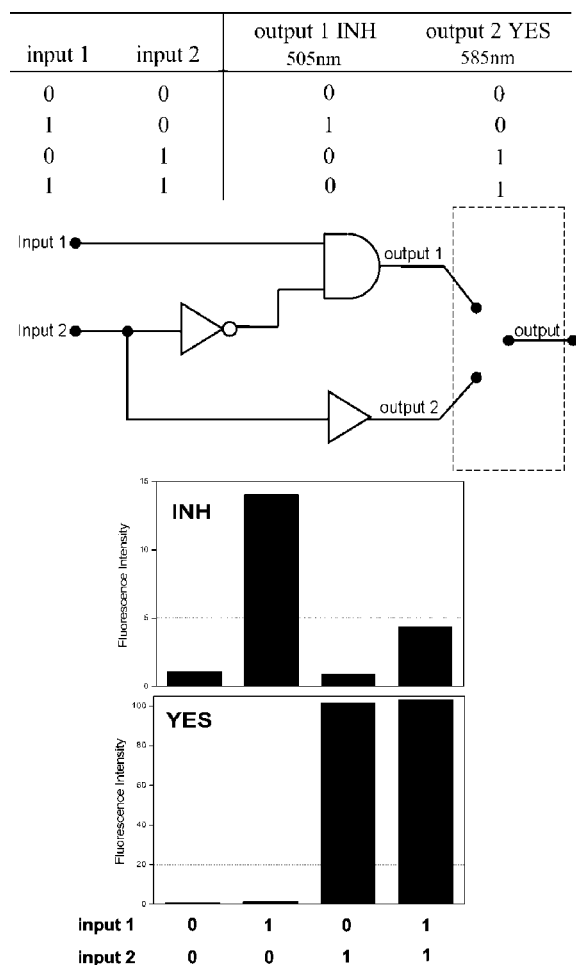


FIGURE 7. Truth table and logic diagram of the combinational logic circuit.

communicative nor associative, it can be viewed as a two-input AND gate, one of whose input lines containing an inverter. However, output 2 results in a YES logic gate (transmission of the input 2 signal to the output neglecting input 1).<sup>17</sup> So the strength of the INHIBIT gate is acknowledged in combination with a YES gate to lead to the construction of a combinational logic circuit.

## Conclusions

We demonstrated a new concept for the selective detection of  $\text{Hg}^{2+}$  and  $\text{Ba}^{2+}$  ions by controlling a logic gate. The characteristic fluorescence of the  $\text{Ba}^{2+}$ -selective OFF–ON and the  $\text{Hg}^{2+}$ -selective fluorescence bathochromic shift can be observed, and these have been used to construct a combinational logic circuit at the molecular level. These results will be useful for further molecular design to mimic the function of the complex logic gates. Due to its flexible structural property, more function groups will attach to calix[4]arene, which is then used to construct more complex logic gates. The work toward this end is in progress.

## Experimental Section

General methods are provide as supporting information.<sup>18–20</sup>

**N-(Rhodamine-B)lactam-ethyl-2-chloroacetamide (3).** In a 100 mL flask, *N*-(rhodamine-B)lactam-ethylenediamine (968 mg, 2.0 mmol) was dissolved in 40 mL of anhydrous dichloromethane, then the solution was cooled with a cold water bath. 2-Chloroacetyl chloride (0.15 mL, little excess) was dissolved in 20 mL of anhydrous dichloromethane and then added dropwise to the flask with vigorous stirring. After the addition, the mixture was allowed to stand in the cold water bath for about 1 h then 0.1 N NaOH (10 mL) was added with stirring until the pH of the solution reached 8–9. Exacted with  $\text{CH}_2\text{Cl}_2$ , the organic phase was washed with water ( $3 \times 20$  mL) and then dried over anhydrous  $\text{Na}_2\text{SO}_4$ . After concentration under vacuum, the residue was purified by column chromatography (silica gel,  $\text{CH}_2\text{Cl}_2/\text{MeOH} = 20:1$ ) to afford a colorless solid (1.03 g, 92%).  $^1\text{H}$  NMR (400 MHz,  $\text{CDCl}_3$ )  $\delta$  7.92 (m, 1H), 7.67 (s, 1H), 7.45 (m, 2H), 7.08 (m, 1H), 6.43 (d, 2H,  $J = 8.8$  Hz), 6.29 (s, 2H), 6.28 (d, 2H,  $J = 8.8$  Hz), 3.92 (s, 2H), 3.34 (m, 10H), 3.09 (t, 2H,  $J = 5$  Hz), 1.19 (t, 12H,  $J = 7$  Hz);  $^{13}\text{C}$  NMR  $\delta$  169.6, 166.2, 153.7, 153.3, 148.9, 132.8, 130.5, 128.4, 128.2, 123.9, 122.9, 108.2, 104.8, 97.8, 65.4, 44.3, 42.3, 40.5, 39.6, 12.6; EI MS  $m/z$  560.0, calcd 561.26; EI MS  $m/z$  561.2636, calcd 561.2554

**4,4-Difluoro-8-{3,4-Bis(2-[2-(*p*-toluenesulfonyloxy)ethoxy]ethoxy)jethoxy)-formylphenyl}-1,3,5,7-tetramethyl-4-bora-3a,4a-diaza-s-indacene (5).** 3,4-Bis(2-[2-(*p*-toluenesulfonyloxy)ethoxy]ethoxy)benzaldehyde (2488 mg, 4 mmol) and 2,4-dimethylpyrrole (761.2 mg, 8 mmol) were dissolved in anhydrous  $\text{CH}_2\text{Cl}_2$  (500 mL) under  $\text{N}_2$  atmosphere. One drop of trifluoroacetic acid was added, and the solution was stirred at room temperature for 5 h. A solution of 2,3-dichloro-5,6-dicyano-1,4-benzoquinone (908 mg, 4 mmol) in anhydrous  $\text{CH}_2\text{Cl}_2$  (100 mL) was added by syringe, and the resulting solution was stirred for 1 h followed by addition of 8 mL of triethylamine and 8 mL of  $\text{BF}_3 \cdot \text{Et}_2\text{O}$ . After being stirred for another 30 min the reaction mixture was washed with water ( $3 \times 100$  mL), and the organic phase was dried over anhydrous  $\text{Na}_2\text{SO}_4$ . After concentration under vacuum, the residue was purified by column chromatography (silica gel,  $\text{CH}_2\text{Cl}_2/\text{AcOEt} = 20:1$ ) to afford a orange-red solid (1.11 g, 33%).  $^1\text{H}$  NMR (400 MHz,  $\text{CDCl}_3$ )  $\delta$  7.79 (t, 4H,  $J = 8.9$  Hz), 7.32 (t, 4H,  $J = 8.0$  Hz), 6.97 (d, 1H,  $J = 8.2$  Hz), 6.81 (m, 2H), 5.98 (s, 2H), 4.17 (m, 6H), 4.04 (d, 2H,  $J = 4.9$  Hz), 3.86 (d, 2H,  $J = 4.9$  Hz), 3.78 (m, 6H), 2.55 (s, 6H), 2.42 (d, 6H,  $J = 7.3$  Hz), 1.46 (s, 6H).  $^{13}\text{C}$  NMR  $\delta$  155.5, 149.5, 149.4, 144.9, 143.2, 141.4, 132.9, 131.7, 129.9, 128, 127.8, 121.2, 114.5, 114.1, 69.8, 69.4, 69.3, 69.1, 69, 68.7, 60.4, 21.7, 21.6, 14.6, 14.5; MALDI MS  $m/z$  878.9 ( $\text{M} + \text{Na}^+$ ), calcd 856.3. Elemental Anal. Calcd for  $\text{C}_{42}\text{H}_{51}\text{BF}_2\text{N}_2\text{O}_{10}\text{S}_2$  (856.3): C, 58.88; H, 6.00; N, 3.27. Found: C, 58.62; H, 6.28; N, 2.89.

(19) Gutsche, C. D.; Levine, J. A.; Sujeeth, P. K. *J. Org. Chem.* **1985**, *50*, 5802.

(20) Cantrill, S. J.; Youn, G. J.; Stoddart, J. F.; Williams, D. J. *J. Org. Chem.* **2001**, *66*, 6857.

(17) Szacilowski, K.; Macyk, W.; Stochel, G. *J. Am. Chem. Soc.* **2006**, *128*, 4550.

(18) Wu, J.; Hwang, I.; Kim, K. S.; Kim, J. S. *Org. Lett.* **2007**, *9*, 907.

**25,27-Dihydroxycalix[4]arene-crown-6-BODIPY, Cone (6).** To a stirred and refluxing solution of 25,26,27,28-tetrahydroxy calix[4]arene (909 mg, 2.14 mmol) and *t*-BuOK (483 mg, 4.3 mmol) in dry benzene (300 mL) was added dropwise compound **4** (1800 mg, 2.14 mmol) in dry benzene (100 mL) over a period of 6 h. After 3 days of refluxing, the reaction mixture was cooled and treated with 10% HCl. The organic layer was washed with water (2 × 100 mL) and dried over anhydrous Na<sub>2</sub>SO<sub>4</sub>, and the solvents were removed under vacuum. The crude product was purified by column chromatography (silica gel, CH<sub>2</sub>Cl<sub>2</sub>/AcOEt = 10:1) to afford an orange-red solid (790 mg, 40%). <sup>1</sup>H NMR (400 MHz, CDCl<sub>3</sub>) δ 7.73 (s, 2H), 7.07 (m, 5H), 6.86 (m, 6H), 6.69 (m, 4H), 5.99 (s, 2H), 4.38 (m, 6H), 4.27 (m, 4H), 4.17 (m, 10H), 3.40 (m, 4H, *J* = 6.6 Hz), 2.57 (s, 6H), 1.49 (s, 6H); <sup>13</sup>C NMR δ 171.2, 155.5, 153.3, 152, 151.9, 150.1, 149.9, 143.2, 141.4, 133.1, 131.7, 129.1, 128.4, 128.3, 128.1, 127.8, 126.8, 126.7, 125.6, 125.5, 121.7, 119.9, 116.2, 115.8, 70.8, 7.07, 7.06, 7.04, 70.1, 60.5, 31.2, 21.2, 14.6, 14.5, 14.2; MALDI MS *m/z* 936.2, caclcd 937.4; EI MS *m/z* 937.44053, calcd 937.43986.

**25,27-Bis[*N*-(rhodamine-B)lactam-ethyl-2-chloroacetamide-yl]calix[4]arene-crown-6-BODIPY (1).** Compound **5** (185 mg, 0.2 mmol), compound **1** (337 mg, 0.6 mmol), Cs<sub>2</sub>CO<sub>3</sub> (130 mg, 0.4 mmol), and a catalytic amount of KI were dissolved in anhydrous CH<sub>3</sub>CN (100 mL) under N<sub>2</sub> atmosphere. The solution was heated at 80 °C for 3 days. After the reaction was completed, the solvents were removed under vacuum. Residue was dissolved in CH<sub>2</sub>Cl<sub>2</sub> (200 mL) and then treated with dilute HCl. The organic phase was washed with water (3 × 100 mL), then dried over anhydrous Na<sub>2</sub>SO<sub>4</sub>. After concentration in vacuum, the crude product was

purified by column chromatography (silica gel, CH<sub>2</sub>Cl<sub>2</sub>/CH<sub>3</sub>OH = 20:1) to afford an orange-red solid (102 mg, 20%). <sup>1</sup>H NMR (400 MHz, CDCl<sub>3</sub>) δ 8.22 (s, 1H), 7.93 (m, 1H), 7.41 (m, 2H), 7.08 (m, 3H), 7.03 (d, 1H), 6.85 (m, 3H), 6.65 (m, 4H), 6.55 (m, 7H), 6.54 (d, 1H), 6.34 (s, 2H), 6.18 (m, 2H), 5.94 (d, 2H, *J* = 13.7 Hz), 4.72 (d, 1H), 4.52 (d, 1H), 4.46 (s, 2H), 4.31 (d, 1H), 4.25 (d, 1H), 4.10 (m, 5H), 3.97 (m, 3H), 3.76 (m, 8H), 3.24 (m, 14H), 3.08 (d, 2H), 2.53 (d, 6H, *J* = 9.3 Hz), 1.4 (d, 6H, *J* = 10 Hz), 1.12 (m, 12H); <sup>13</sup>C NMR δ 170.3, 168.7, 154.5, 153.6, 153.5, 153.3, 153.2, 149.2, 148.9, 148.6, 141.8, 135.9, 133.7, 133.5, 133.3, 133.1, 131.3, 129.0, 128.9, 128.8, 128.6, 128.4, 128.0, 126.7, 123.7, 122.6, 118.1, 112.1, 108.0, 106, 105.8, 97.3, 75.5, 7.01, 69.6, 69.4, 68.3, 67.4, 65.3, 53.4, 44.3, 31.0, 30.8, 30.5, 29.8, 15.0, 14.8, 14.6, 14.1, 12.7; MALDI MS *m/z* 1460.6, caclcd 1460.7; EI MS *m/z* 1460.72290, calcd 1460.73273. Elemental Anal. Calcd for C<sub>88</sub>H<sub>95</sub>BF<sub>2</sub>N<sub>6</sub>O<sub>11</sub> (1460.7): C, 72.91; H, 6.48; N, 5.81. Found: C, 72.46; H, 6.85; N, 5.52.

**Acknowledgment.** This work was supported by the National Nature Science Foundation of China (20531060) and the National Basic Research 973 Program of China (Grant Nos. 2006CB932102, 2006CB806200, and 2007CB936401).

**Supporting Information Available:** Time-resolved fluorescence data, NMR spectra, MS spectra, as well as binding analysis for Hg<sup>2+</sup> and Ba<sup>2+</sup>. This material is available free of charge via the Internet at <http://pubs.acs.org>.

JO8005683